



# Chapter 8

## Optimal Sensor Configuration Design for Virtual Sensing in a Wind Turbine Blade Using Information Theory

Tulay Ercan, Konstantinos Tatsis, Victor Flores Terrazas, Eleni Chatzi, and Costas Papadimitriou

**Abstract** Optimal sensor placement (OSP) strategies in complex engineering systems aim to maximize the information gain from data by optimizing the location, type and number of the sensors or the actuators. It is used as a guide for assessing the structural condition, detecting damages and supporting the decision-making regarding structural health, safety and performance. In this work, a Bayesian optimal experimental design framework is used to optimize the type, location and number of sensors in composite wind turbine blades (WTB) excited by wind loads. The framework is based on a modal expansion technique for virtual sensing under output-only vibration measurements and on information theory for quantifying the information contained in a sensor configuration. The optimal sensor configuration optimizes a utility function associated with the expected Kullback-Leibler divergence (KL-div) between the prior and posterior distribution of the predictions at the virtual sensing (Ercan and Papadimitriou, *Sensors* 21:3400, 2021). The design variables include the location, type and number of sensors.

**Keywords** Bayesian optimal experimental design · Information gain · Virtual sensing · Modal expansion · Wind turbines

### 8.1 Analysis

Employing the Gaussian nature of the response estimates for a linear model of the WTB, the utility function is formulated in terms of the prior and posterior covariance matrices of the error in the estimates of the response predictions. The optimal sensor placement theory and tools are presented in reference [1]. Specifically, using the expected KL-div between the prior and posterior distribution of the output quantities of interest (QoI) to be reliably predicted using the measurements, the utility function which quantifies the information gained from a sensor configuration is finally derived in the form

$$U(\delta) = -\frac{1}{2} \sum_{i=1}^{n_z} \ln \left[ \underline{\psi}_i^T \left[ \Phi^T L^T(\delta) Q_e^{-1}(\delta) L(\delta) \Phi + S^{-1} \right]^{-1} \underline{\psi}_i + Q_{\varepsilon_i} \right] / \left[ \underline{\psi}_i^T S \underline{\psi}_i + Q_{\varepsilon_i} \right] \quad (8.1)$$

where  $\Phi \in R^n \times m$  is the full displacement modeshape matrix associated with all degrees of freedom (DOF) of the model,  $L(\delta)$  is the observation matrix that maps the displacements at all  $n$  DOF to the measured displacement or strain quantities indicated in the sensor location vector  $\delta \in R^{N_0}$  containing the sensor “location” information (DOF for displacement sensors; positions and directions for strain sensors),  $\underline{\psi}_i$  is the  $i$ -th row of the modeshape matrix  $\Psi \in R^{n_z \times m}$  associated with the type of predictions (e.g. strain modeshapes for the case of strain predictions),  $\Psi \in R^{n_z \times m}$  contains the modeshape components at the

---

T. Ercan · C. Papadimitriou (✉)  
Department of Mechanical Engineering, University of Thessaly, Volos, Greece  
e-mail: [ercan@uth.gr](mailto:ercan@uth.gr); [costasp@uth.gr](mailto:costasp@uth.gr)

K. Tatsis · E. Chatzi  
Department of Civil, Environmental and Geomatic Engineering, Institute of Structural Engineering, Zürich, Switzerland  
e-mail: [tatsis@ibk.baug.ethz.ch](mailto:tatsis@ibk.baug.ethz.ch); [chatzi@ibk.baug.ethz.ch](mailto:chatzi@ibk.baug.ethz.ch)

V. F. Terrazas  
Department of Civil and Environmental Engineering, The Hong Kong University of Science and Technology, Hong Kong, China  
e-mail: [vft@connect.ust.hk](mailto:vft@connect.ust.hk)

$n_z$  locations where predictions are made,  $m$  is the number of contributing modes and  $N_0$  is the number of sensors involved in the sensor configuration. The quantity  $Q_e = s^2 I + \sigma_e^2 \tilde{Q}_y$  represents the covariance matrix of the total predictions error with  $s$  accounting for the intensity of the measurement error and  $\sigma_e$  accounting for the intensity of the model error with respect to the intensity of the responses at the measured locations, and  $\tilde{Q}_y$  is the diagonal matrix containing at the diagonals the variances of the measured responses  $\underline{y}(t) \in R^{N_0}$  at the measured locations. The quantity  $Q_{\varepsilon_i} = \sigma_e^2 \tilde{Q}_{z_i}$  denotes the variance of the prediction error expected for the predicted response quantity  $z_i(t)$ , where  $\tilde{Q}_{z_i}$  is the diagonal matrix containing at the diagonals the variances of the predicted time history  $z_i(t)$ . The quantity  $S = \alpha^2 \tilde{Q}_\xi$  is the covariance of the prior distribution assumed for the modal quantities  $\underline{\xi}(t)$ , where  $\alpha$  quantifies the extent of uncertainty in the prior distribution. The optimal  $\underline{\delta}$  is selected as the one that maximizes  $U(\underline{\delta})$ . Both a genetic algorithm (GA) and alternative heuristic sequential sensor placement (SSP) algorithms are used to solve the optimization problem in an effort to provide computationally efficient solutions.

## 8.2 Application

The OSP methodology is applied to a small-scale composite WTB structure. The structure with its structural and geometrical properties as well as the monitoring campaign performed at ETH Zurich is presented in detail in references [2, 3]. A simple representation of the WTB can be seen in Fig. 8.1. The blade model is fixed at the left edge and the outer surface consists of 6189528 nodes and 242930 six-degree-of-freedom thin shell elements. OSP analysis is performed to optimize the location and number of strain sensors for strain response prediction on the locations marked with red dots in Fig. 8.1. For illustration purposes, it is assumed that the blade is subjected to a point load defined as a white noise input with a sampling period  $\Delta t = 0.0025$  sec at the location shown in Fig. 8.1. The OSP design is performed assuming eight contributing modes. Model and measurement error parameters  $\sigma_e$  and  $s$  (see [1] for details) are selected according to the intensities of responses (of the observed QoI) and given in Table 8.1 with the prior parameter  $\alpha$  and the prediction error parameter  $\sigma_\varepsilon = \sigma_e$ . The values in Table 8.1 correspond to small model error of the order of 1%, as well as medium to small measurement error ranging from 20% to 0.4% measurement error for the minimum and maximum reported strain in the structure.

The OSP results for strain sensors are presented in Fig. 8.2. The expected information gain (utility values) as a function of the number of sensors placed at their optimal (or worst) locations is shown in Fig. 8.2a, while the optimal positions of eight sensors are shown in Fig. 8.2b. The maximum utility value ( $U_{\max} = 9.17$ ) which can be reached with 245 strain sensors is shown as a grey horizontal line in Fig. 8.2a. For less than eight sensors (the number of contributing modes), the problem of OSP is unidentifiable, and subjective information for placing sensors is borrowed from the prior PDF.

As a result, the information gain for a configuration up to 7 sensors is significantly less than the maximum information gain that can be achieved with 245 strain sensors uniformly spread over the blade surface. Including eight sensors in the sensor configuration leads to a sharp increase in the information gain, reaching a value which is very close to the maximum information gain. Adding more than eight sensors at the optimal locations results in a relatively small increase in information gain. From the optimal sensor configuration results in Fig. 8.2b, it can be seen that the strain sensors are well distributed along the blade for reliable response prediction. For validation purposes, strain responses at the 245 locations shown in Fig. 8.1 are predicted from the modal expansion technique by using the best, worst and an arbitrary sensor configuration, all involving eight sensors. For this, simulated measurement data are generated at all 245 strain locations using white noise input

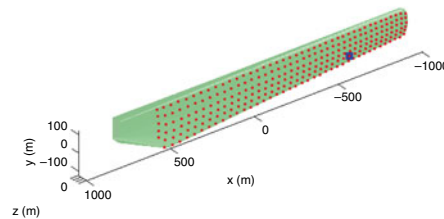


Fig. 8.1 Location of input (blue), predictions and possible sensors (red)

Table 8.1 Prior, prediction error, model and measurement error parameters

Sensor type	$\alpha$	$\sigma_\varepsilon$	$\sigma_{em}$	$s$	$\sim s/\varepsilon_{min}$	$\sim s/\varepsilon_{max}$
Strain	$10^2$	$10^{-2}$	$10^{-2}$	$10^{-7}$	$2 \times 10^{-1}$	$4 \times 10^{-3}$

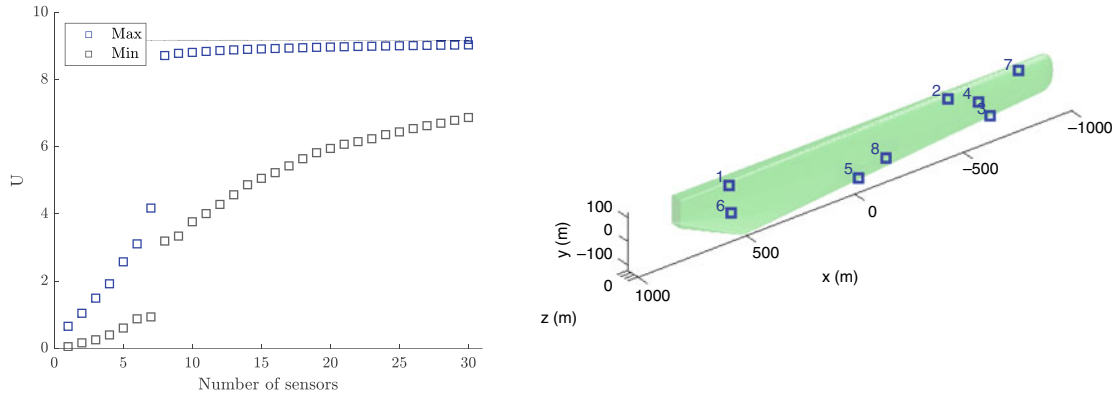


Fig. 8.2 OSP results – utility values (a), best sensor positions (b)

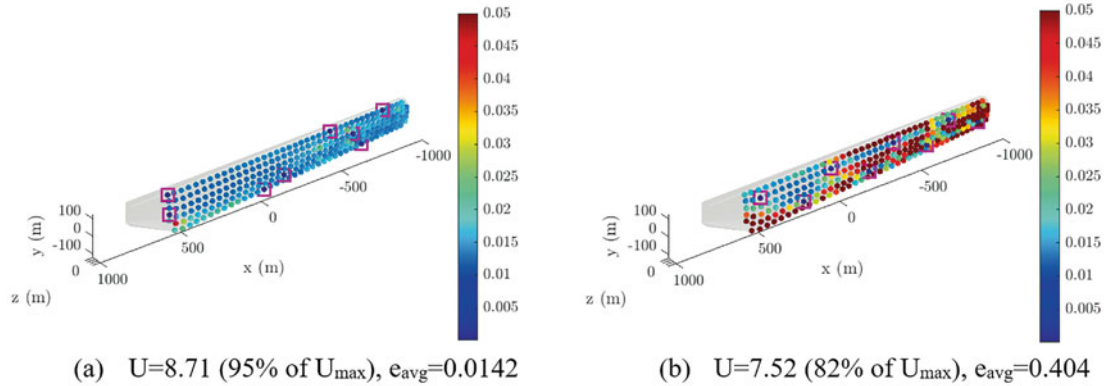


Fig. 8.3 Relative error in response prediction locations using best (a) and arbitrary (b) sensor locations. Magenta shows measured locations

at the input location shown in Fig. 8.1. 1% of the intensity of the strains is added as Gaussian noise in the simulated response time histories to include model and measurement error. Given these simulated measurements, the OSP methodology is used to predict responses in measured and unmeasured locations from the three different sensor configurations involving eight strain sensors. Relative root mean square (RRMS) errors between the predictions and the simulated measurements for the two sensor configurations (with their utility values) are presented in Fig. 8.3.

Very good predictions with average RRMS error equal to 0.0142 and maximum RRMS error less than 0.03 are obtained with the optimal sensor configuration. With the worst sensor locations, the average RRMS error (not shown in the figure) in the unmeasured locations is 180%, much higher than the one found with the best locations. The results also indicate that the selected arbitrary sensor layout, corresponding to a utility value that is approximately 20% less than the utility value for the optimal sensor configuration, also give a higher average RRMS error of 40% in the response prediction in the unmeasured locations.

### 8.3 Conclusions

The OSP approach is applicable for studying the effects of uncertainties in measurement and model errors, the temporal and spatial distribution of loads and the prior distribution on the optimal sensor configuration design. These studies are important to demonstrate the capabilities of the proposed OSP framework for WTB operating in a highly dynamic and uncertain environment. The proposed framework is applicable to optimize the experimental design for a wide variety of systems that require comprehensive use of limited resources in the experiment due to the high cost of maintenance and inspection.

**Acknowledgements** This project has received funding from the European Union’s Horizon 2020 research and innovation programme under the Marie Skłodowska-Curie grant agreement No 764547.

## References

1. Ercan, T., Papadimitriou, C.: Optimal sensor placement for reliable virtual sensing using modal expansion and information theory. *Sensors*. **21**(10), 3400 (2021)
2. Ou, Y., Tatsis, K.E., Dertimanis, V.K., Spiridonakos, M.D., Chatzi, E.N.: Vibration-based monitoring of a small-scale wind turbine blade under varying climate conditions. Part I: an experimental benchmark. *Struct. Control. Health Monit.* **28**(6), e2660 (2021)
3. Tatsis, K., Ou, Y., Dertimanis, V.K., Spiridonakos M.D., Chatzi, E.N.: Vibration-based monitoring of a small-scale wind turbine blade under varying climate and operational conditions. Part II: a numerical benchmark. *Struct. Control. Health Monit.* **28**, e2734 (2021)